31st Annual International Conference of the IEEE EMBS
Minneapolis, Minnesota, USA, September 2-6, 2009

Nonlinear Model of Single Hippocampal Neurons with Dynamical Thresholds

Ude Lu, *Student Member*, Dong Song, *Member*, and Theodore W. Berger, *Senior Member, IEEE*

***Abstract*—Neurons transform a series of presynaptic spikes into a series of postsynaptic spikes through a number of nonlinear mechanisms. A nonlinear model with a dynamical threshold was built using a Volterra Laguerre kernel method to characterize the spike train to spike train transformations of hippocampal CA1 pyramidal neurons. Inputs of the model were broadband Poisson random impulse trains with a 2 Hz mean frequency, and outputs of the model were the corresponding evoked post-synaptic potential (PSP) and spike train data recorded from CA1 cell bodies using a whole-cell recording technique. The model consists of four major components, i.e., feedforward kernels representing the transformation of presynaptic spikes to PSPs; a dynamical threshold kernel determining threshold value based on output inter-spike-intervals (ISIs); a spike detector; and a feedback kernel representing the spike-triggered after-potentials.**

I. Introduction

Neurons receive presynaptic spike trains and transform them into postsynaptic spike trains. All cognitive functions such as perception, language, emotion, learning, and memory are embedded in neuron spike train to spike train temporal pattern transformations. It is important to understand the neuron transformations as well as to computationally reproduce the output patterns given the input patterns [1].

The nonlinear dynamical single neuron modeling based on Volterra kernels appears to be important in two ways. First, it captures the neuron nonlinear transformations based on neuron input-output relationships without the bias of partial knowledge. Bias of partial knowledge is almost unavoidable in compartmental modeling by nature [2]. Second, the model developed in this report provide real time prediction. This computational efficiency is important for future development of large scale simulations.

The inputs of the model used in this report are Poisson random interval spike trains sent to Schaffer collaterals, one of the major afferents to CA1 pyramidal neurons. The Poisson random interval stimulation trains with 2Hz mean frequency include the majority of spike train patterns observed in behaving rats, and can induce physiologically plausible nonlinearities. The outputs of the model are whole-cell recordings of CA1 pyramidal neurons. Whole-cell recordings enable us to access detailed sub-threshold PSPs reflecting the characterization of sub-threshold nonlinearities, and detailed action potential waveforms reflecting active conductances originated from multiple sources, allowing threshold measurements of each individual action potential.

Like many other neurons in the CNS, hippocampal CA1 pyramidal neurons receive tens of thousands of excitatory synaptic contacts over their dendritic arborizations. Many single neuron processes are nonlinear, such as presynaptic neurotransmitter releasing, postsynaptic dendritic integrations, somatic integrations, and spike generations [3, 4].

The up to 3rd order feedforward Volterra kernels in the model developed in this report characterized the nonlinear transformation from presynaptic spikes to pre-threshold PSPs. Once the pre-threshold PSPs are over the threshold, the action potentials are induced. Threshold has generally been taken for granted to be a constant. However, taken the evidence from literature and our data, we like to argue that threshold is not a constant and it is important to include threshold dynamics to produce accurate spike predictions. In 2001, Henze and Buzsáki proposed and applied third derivative method to measure the threshold of each action potential of *in vivo* intracellularly recorded data. They showed that there was inverse relationships between the length of the inter-spike-intervals (ISIs) and amplitudes of thresholds: the shorter the ISI, the higher the threshold amplitudes. This phenomena has also been confirmed in this report using the same measuring method and CA1 whole-cell recording data, which will be described in detail in the methods section. To address that issue, we built a third-order nonlinear threshold model in addition to the previously developed model structure to characterize threshold dynamical behaviors and to improve spike prediction accuracy [5].

II. Materials and Methods

A. Electrophysiology

Hippocampal slices were prepared from male, juvenile Sprague-Dawley rats (14-21 days of age). Animals first were anesthetized with 5% halothane, and then were decapitated and the hippocampi were rapidly dissected. Both hippocampi

Manuscript received May, 2009. This work was supported by NSF, DARPA (HAND), and NIH (NIBIB).

Ude Lu is with the Department of Biomedical Engineering, University of Southern California, Los Angeles, CA 90089 USA (phone: 213-740-8063; fax: 213-740-8061; e-mail: ulu@ usc.edu).

Dong Song is with the Department of Biomedical Engineering, University of Southern California, Los Angeles, CA 90089 USA (e-mail: dsong@usc.edu).

Theodore W. Berger is with the Department of Biomedical Engineering, University of Southern California, Los Angeles, CA 90089 USA (e-mail: berger@bmsr.usc.edu).

were sectioned into blocks while being washed with cold, oxygenated medium. Slices of tissue (400 microns thick) then were cut perpendicular to the longitudinal axis using a vibratome. Slices were incubated with medium consisting of (in mM): 128 NaCl; 2.5 KCl; 1.25 NaH_2PO_4; 26 $NaHCO_3$; 10 Glucose; 1 $MgSO_4$, 2 Ascorbic Acid, and 1 $CaCl_2$ with pH 7.4 and 295 mOsmol. Based on visible and consistent anatomical boundaries, a bipolar nichrome stimulating electrode was placed so as to activate Schaffer collaterals (Fig. 1a and b), a major excitatory afferent to CA1 pyramidal cells. PSPs were consistently evoked by Poisson random impulse train stimulation with 2Hz mean frequency and recorded with whole-cell recording process with glass tip resistances of approximately 4MΩ (Fig. 1a and c) and internal solution (in mM): 110 Potassium-Gluconate, 10 HEPES, 1 EGTA, 20 KCl, 4 NaCl, 2 Mg-ATP, and 0.25 Na_3-GTP with pH 7.3, 290 mOsmol.

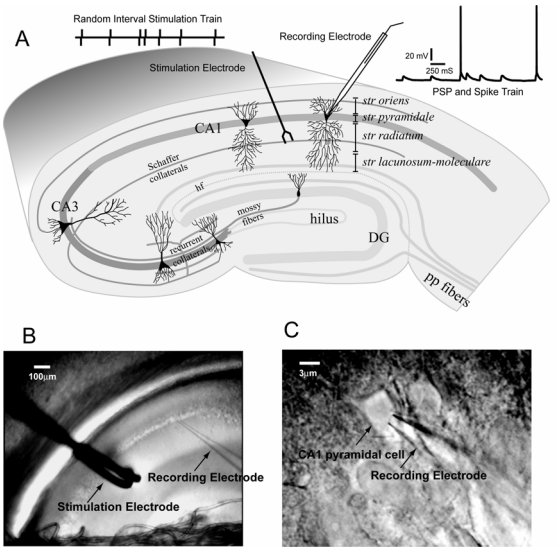

Figure 1. Hippocampus slice anatomy and experimental paradigm (a). Picture showing relative position of stimulation electrode and recording electrode with respect to the CA1 region of the hippocampal slice (b). Low magnification photomicrograph (40x) showing stimulating electrode in the s. radiatum of the CA1, and a fine glass micropipette approaching the pyramidal cell layer. High magnification photomicrograph (400x) showing recording electrode patching onto CA1 pyramidal cell soma (c).

B. Threshold Dynamics

1) Threshold Measurement:

Many different threshold measuring methods have been suggested [6]. In this report, we applied the method proposed by Henze and Buzsáki in 2001. They suggested that thresholds are the voltage values of the PSPs corresponding to the first peak of 3rd derivatives of PSPs [7]. Please see Figure 2. The third derivative equation is expressed as following,

$$\frac{d^3V_t}{dt^3} \approx \frac{V_{t-3} - 8V_{t-2} + 13V_{t-1} - 13V_{t+1} + 8V_{t+2} - V_{t+3}}{8\Delta t^3} \quad (1)$$

This estimation is derived from Taylor series expansions to be accurate to $O(\Delta t^4)$ [8].

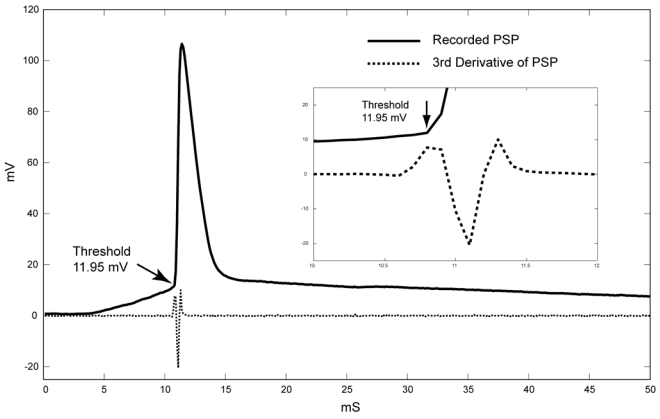

Figure 2. Threshold measuring process. The voltage value of PSP corresponding to the first peak of 3rd derivative of PSP is calculated to be the threshold.

2) Threshold vs. Inter-Spike-Interval:

Plotting the threshold analysis from our data shows that shorter inter-spike-interval are associated with increased spike thresholds. Please see Figure 3.

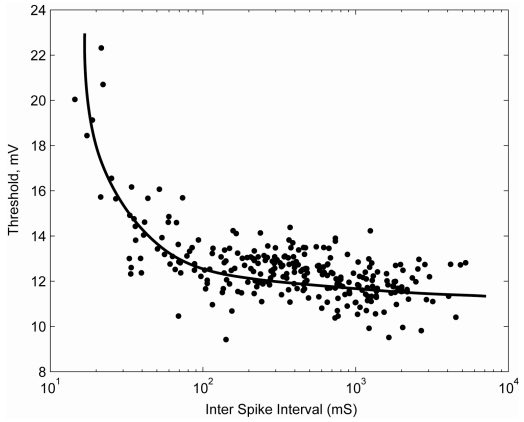

Figure 3. Threshold value vs. inter-spike-interval.

C. Laguerre Volterra Modeling

The overall model structure is shown in Figure 4, and represents an extension of a model first proposed by Dong et al., 2007 [3]. The model consist three Volterra kernels and a spike detector.

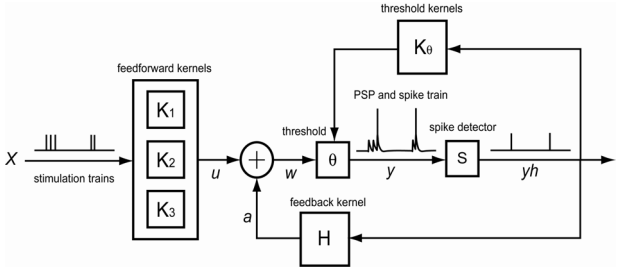

Figure 4. Model structure.

In Figure 4,

$$w = u(k,x) + a(h,yh) \quad (2)$$

$$y = \begin{cases} \text{action potential} & ,w \geq \theta \\ w & ,w < \theta \end{cases} \quad (3)$$

where, x is the presynaptic stimulation train as well as input of

the feedforward kernel; *u* represents pre-threshold PSPs as well as the feedforward kernel output; *w* is the summation of *u* and *a*; *y* represents the somatic PSPs and spike train as well as the overall model output; *yh* represents the extracted spike information from *y*; and *a* represents the spike triggered after potential contributions.

1) Feedforward Kernels:

The feedforward pre-threshold PSPs, *u,* were expressed with the Laguerre Volterra method in the following way,

$$\begin{aligned} u(t) = c_{k_0} &+ \sum_{j=1}^{L} c_{k_1}(j) v_j^{k_1}(t) \\ &+ \sum_{j_1=1}^{L}\sum_{j_2=1}^{j_1} c_{k_2}(j_1, j_2) v_{j_1}^{k_2}(t) v_{j_2}^{k_2}(t) \\ &+ \sum_{j_1=1}^{L}\sum_{j_2=1}^{j_1}\sum_{j_3=1}^{j_2} c_{k_3}(j_1, j_2, j_3) v_{j_1}^{k_3}(t) v_{j_2}^{k_3}(t) v_{j_3}^{k_3}(t) \end{aligned} \tag{4}$$

in which,

$$v_j^k(t) = \sum_{\tau=0}^{M_k} b_j^k(\tau) x(t-\tau) \tag{5}$$

In the equation, *L* denotes the number of Laguerre basis functions; c_{k_0}, c_{k_1}, c_{k_2}, and c_{k_3} are the open parameters for the feedforward kernels k_0, k_1, k_2, and k_3 that were optimized with least square estimation; M_k is memory window; and $v_j^k(t)$ is the convolution of Laguerre basis functions of feedforward kernels b_j^k and input *x(t)*.

2) Feedback Kernels:

The spike triggered feedback contribution *a(t)* could be expressed in the following way,

$$a(t) = \sum_{j=1}^{L} c_h(j) v_j^h(t) \tag{6}$$

in which,

$$v_j^h(t) = \sum_{\tau=1}^{M_h} b_j^h(\tau) yh(t-\tau) \tag{7}$$

where, c_h represent open parameters of feedback kernel *H*; M_h is memory window; $v_j^h(t)$ is the convolution of Laguerre basis functions of feedback kernels b_j^h and output spike train *yh*. The expression of *yh* is as follows,

$$yh = \begin{cases} 1 & , y \text{ is action potential} \\ 0 & , y = w \end{cases} \tag{8}$$

3) Threshold Kernels:

The threshold θ in Figure 4 is expressed as following,

$$\theta(n) = c_{\theta_1} + \sum_{j=1}^{L} c_{\theta_2}(j) v_j^{\theta_2}(n) + \sum_{j_1=1}^{L}\sum_{j_2=1}^{j_1} c_{\theta_3}(j_1, j_2) v_{j_1}^{\theta_3}(n) v_{j_2}^{\theta_3}(n) \tag{9}$$

where,

$$v_j^\theta(n) = \sum_{m=0}^{M_\theta} b_j^\theta(m) yh(t_n - m) \tag{10}$$

in which, n is the numerical sequence of input pulses, *x*; t_n is the time corresponding n-th input in x; m is time lag within memory window; M_θ is the memory window size. $v_j^\theta(n)$ is the convolution of Laguerre basis functions of dynamic threshold kernels b_j^h and output spike train *yh*. Thresholds are scalars not like PSPs are 2D waveforms. This makes threshold kernels one order lower than PSPs feedforward and/or feedback kernels.

D. Kernel Constructions

Volterra kernels were reconstructed with the optimized Laguerre coefficients c_k, c_h, and c_θ in the following way,

Feedforward kernels

$$k_{i,1\le i\le 3}(\tau_1, ..., \tau_i) = \sum_{j_1=1}^{L} ... \sum_{j_i=1}^{L} c_{k_i}(j_1, ..., j_i) b_{j_1}^k(\tau_1) ... b_{j_i}^k(\tau_i) \tag{11}$$

Feedback kernel

$$h(\tau) = \sum_{j=1}^{L} c_h(j) b_j^h(\tau) \tag{12}$$

Dynamic threshold kernels

$$k_1^\theta = c_{\theta_1} \tag{13}$$

$$k_{i,2\le i\le 3}^\theta(m_1, \cdots, m_{i-1}) = \sum_{j_1=1}^{L} \cdots \sum_{j_{i-1}=1}^{L} c_{\theta_{i-1}}(j_1, \cdots, j_{i-1}) b_{j_1}^\theta(m_1) \cdots b_{j_{i-1}}^\theta(m_{i-1}) \tag{14}$$

For electrophysiological interpretations of Volterra kernels please see result section and Song, 2009 [2].

E. Model Evaluations

Normalized mean square error (NMSE) was used to evaluate the PSPs waveform prediction, which is expressed as following,

$$NMSE = \sum_{n=1}^{N} (y(n) - t(n))^2 / \sum_{n=1}^{N} t(n)^2 \tag{15}$$

where *y(n)* represent recorded data, *t(n)* represent prediction data.

Spike prediction error rate (SPER) was applied to evaluate spike prediction accuracy, defined as following,

$$\text{SPER} = \frac{\text{Numbers of False Positive + Numbers of True Negative}}{\text{Total Number of Stimulations}} \tag{16}$$

III. RESULT

A. Prediction Result with a Constant Threshold

Sample clips of data set of CA1 pyramidal cell whole-cell recorded original PSPs and model predicted PSPs with constant threshold are shown in Figure 5.

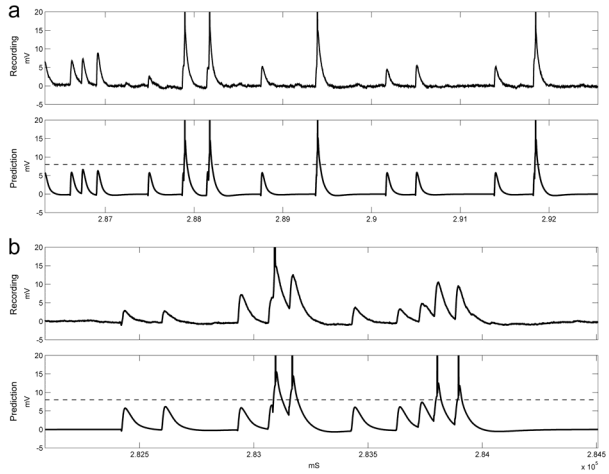

Figure 5. Sample data of whole-cell PSPs recording and out-sample prediction. Sample clip that the prediction accurately match the recording (a). Sample clip that produce false-positive spike prediction (b).

The prediction with constant threshold was done in two steps. First, the optimized open parameters of feedforward and feedback kernels were trained simultaneously to produce the minimum normalized mean square error (NMSE). Second, receiver operating curve (ROC) were used to find an optimal constant threshold.

As shown in Figure 5b, the model predictions produce some false-positive prediction error. It was exactly this kind of imperfect spike prediction that inspired us to construct a dynamic threshold model.

B. Feedforward and Feedback Kernels

Up to third order feedforward kernels and one first-order feedback kernel are shown in Figure 6.

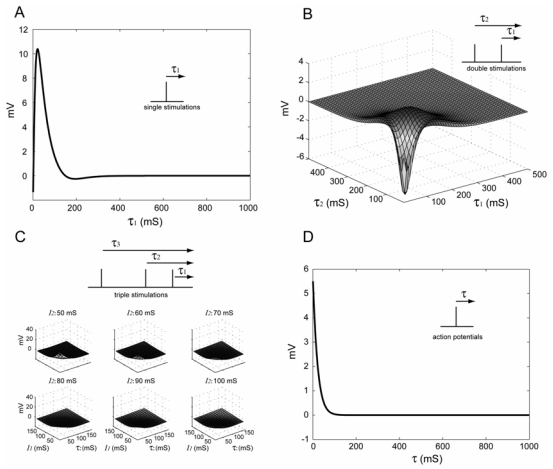

Figure 6. Feedforward and feedback kernels. First order feedforward kernel (A). Second order feedforward kernel (B). Third order feedforward kernel (C). Feedback kernel (D).

Mathematically, the first order feedforward kernel (Figure 6a) works as a linear filter and could be viewed as the impulse response of the neuron PSPs. Physiologically, the first order kernel describes the neuron response to an isolated stimulation.

In the case of multiple stimulations, on top of first order feedforward kernel, the second order kernel (Figure 6b) describes the nonlinear dynamics of how, within the memory window, a previous single stimulation affects the current output. The second response will be the summation of first order kernel and second order kernel given the right stimulation interval I_1. Up from second order kernel, time or use dependent nonlinearity is introduced.

Similar to second order kernel, third order kernel (Figure 6c) shows how two combined previous stimulations together, within the memory window, affect the response of current stimulation. In the up to 3rd order model, the response for current stimulation is the total sum of first order kernel of the current stimulation itself, second order kernel contributed by each of the previous stimulations, and third order kernel contributed by the each of the paring combinations of previous stimulations.

Feedback kernel describes the spike triggered after potential contribution (Figure 6d).

C. Dynamical Threshold Kernels

The reconstructed threshold kernels are shown in Figure 7.

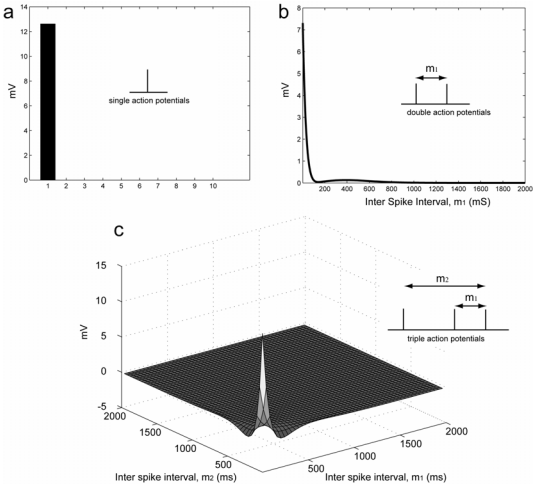

Figure 7. Dynamic threshold kernels. First order threshold kernel (a). Second order threshold kernel (b). Third order threshold kernel (c).

Thresholds are values, not like PSPs are two dimensional waveforms. So, the first order threshold kernel is a scalar as shown in Figure 7a. We name the order of kernels according to how many inputs are considered instead of the dimension of convolutions. Physiologically, first order kernel is the expected threshold value to an isolated stimulation. Second order threshold kernel, shown in Figure 7b, represent the effect of previous spike on current response. The second order threshold kernel shows that if the inter-spike-interval is shorter then 100 mS, the threshold for current response will be much higher than previous spike. In a similar sense, third order threshold kernel, shown in Figure 7c, describes the effect of every pair of previous spike on current response.

The result of threshold prediction is shown in Figure 8.

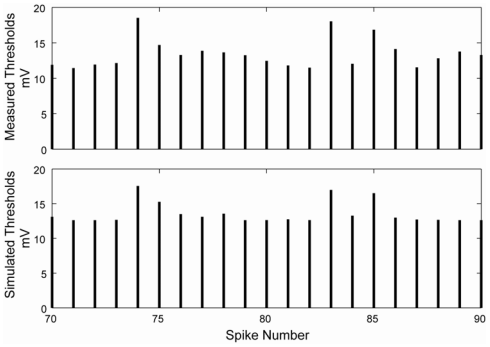

Figure 8. Threshold predictions. Measured thresholds from recorded data (upper panel). Model predicted thresholds (lower panel).

IV. Discussion

Originally, we build our model without the dynamic threshold kernels. Statistical analysis of the prediction performance were evaluated in two ways: 1) normalized mean square error (NMSE), comparing the error between

recorded and predicted pre-threshold PSPs; 2) spike prediction error rate (SPER), which is the total number of false-positive and true-negative in spike predictions over the total numbers of presynaptic stimulations. The average performance of NMSE and SPER over 16 cells from different animals were both close to 20% (data not shown). The intention to improve the SPER motivated the idea of building a dynamical threshold. As shown in the result section, the model has been constructed. However, we have not integrated the dynamic threshold thoroughly into the model to perform iterative real time prediction as we did with constant threshold. The work is still under construction.

In summary, our model, which is the first of the kind, characterizes the nonlinearity of sub-threshold PSPs and threshold dynamics of single neurons. Hence, our model has broad implications not only in engineering but also in neuroscience.

REFERENCES

[1] W. Gerstner and W. Kistler, *Spiking Neuron Models*: Cambridge, 2002.

[2] D. Song, V. Z. Marmarelis, and T. W. Berger, "Parametric and non-parametric modeling of short-term synaptic plasticity. Part I: Computational study," *Journal of computational neuroscience*, vol. 26, pp. 1-19, 2009.

[3] D. Song, R. H. Chan, V. Z. Marmarelis, R. E. Hampson, S. A. Deadwyler, and T. W. Berger, "Nonlinear dynamic modeling of spike train transformations for hippocampal-cortical prostheses," *IEEE Trans Biomed Eng*, vol. 54, pp. 1053-66, 2007.

[4] A. Frick and D. Johnston, "Plasticity of dendritic excitability," *Journal of Neurobiology*, vol. 64, pp. 100-15, 2005.

[5] U. Lu, D. Song, and T. W. Berger, "Nonparametric modeling of single neuron," *30th Annual International Conference of the IEEE EMBS Conference Proceedings.* vol. 2008, pp. 2469-72, 2008.

[6] M. Sekerli, C. A. Del Negro, R. H. Lee, and R. J. Butera, "Estimating action potential thresholds from neuronal time-series: New metrics and evaluation of methodologies," *IEEE Trans Biomed Eng*, vol. 51, pp. 1665-1672, 2004.

[7] D. A. Henze and G. Buzsaki, "Action potential threshold of hippocampal pyramidal cells in vivo is increased by recent spiking activity," *Neuroscience*, vol. 105, pp. 121-30, 2001.

[8] B. Raton, *Standard Mathematical Tables and Formulae*, 29th ed: CRC, 1991.